

## Article

# Online SOC Estimation Based on Simplified Electrochemical Model for Lithium-Ion Batteries Considering Current Bias <sup>†</sup>

Longxing Wu , Kai Liu <sup>\*</sup>, Hui Pang <sup>\*</sup>  and Jiamin Jin

School of Mechanical and Precision Instrument Engineering, Xi'an University of Technology, Xi'an 710048, China; batterywu@163.com (L.W.); 2190221216@stu.xaut.edu.cn (J.J.)

<sup>\*</sup> Correspondence: kliu@xaut.edu.cn (K.L.); huipang@163.com (H.P.); Tel.: +86-29-8231-2599 (H.P.)

<sup>†</sup> This paper is an extended version of our paper presented in International Conference on Electric and Intelligent Vehicles (ICEIV2021), Nanjing, China, 25–28 June 2021.

**Abstract:** State of Charge (SOC) is essential for a smart Battery Management System (BMS). Traditional SOC estimation methods of lithium-ion batteries are usually conducted using battery equivalent circuit models (ECMs) and the impact of current sensor bias on SOC estimation is rarely considered. For this reason, this paper proposes an online SOC estimation based on a simplified electrochemical model (EM) for lithium-ion batteries considering sensor bias. In EM-based SOC estimation structure, the errors from the current sensor bias are addressed by proportional–integral observer. Then, the accuracy of the proposed EM-based SOC estimation is validated under different operating conditions. The results indicate that the proposed method has good performance and high accuracy in SOC estimation for lithium-ion batteries, which facilitates the on-board application in advanced BMS.

**Keywords:** lithium-ion batteries; simplified electrochemical model; state of charge; proportional–integral observer; sensor bias



**Citation:** Wu, L.; Liu, K.; Pang, H.; Jin, J. Online SOC Estimation Based on Simplified Electrochemical Model for Lithium-Ion Batteries Considering Current Bias. *Energies* **2021**, *14*, 5265. <https://doi.org/10.3390/en14175265>

Academic Editor: Carlos Miguel Costa

Received: 30 July 2021

Accepted: 23 August 2021

Published: 25 August 2021

**Publisher's Note:** MDPI stays neutral with regard to jurisdictional claims in published maps and institutional affiliations.



**Copyright:** © 2021 by the authors. Licensee MDPI, Basel, Switzerland. This article is an open access article distributed under the terms and conditions of the Creative Commons Attribution (CC BY) license (<https://creativecommons.org/licenses/by/4.0/>).

## 1. Introduction

With the rapid development of electric vehicles (EVs), the Lithium-ion battery (LIB) has become the most important energy storage device, since it exhibits high energy and power density, along with no memory effect [1]. Because the overcharge or over discharge of LIB will inevitably damage the battery's inner characteristics and state of health (SOH) [2], the state-of-charge (SOC) evaluation of LIB has gradually become one of the important concerns for Battery Management System (BMS), which has attracted a significant amount of researchers' attention.

The existing SOC estimation methods are mainly divided into three categories: basic methods (such as the looking-up table and ampere–hour integral methods), data-driven methods and model-based methods [3]. In contrast to the other two methods, the model-based methods display favourable accuracy and robustness for SOC estimation in BMS due to the closed-loop control and insensitivity to the external disturbances [4]. It is well-known that there are two types of widely used battery models, including equivalent circuit model (ECM) [5,6] and electrochemical model (EM) [7,8]. Due to the simple and flexible structures of ECMs, the extended Kalman filter (EKF) [9–11], Luenberger observers [12,13] and the sliding mode observers [14] were widely applied to estimate SOC based on ECMs. These methods of SOC estimation can obtain acceptable results, yet the calculation complexity is very high as well as it cannot reflect the variation of the SOC from the battery internal characteristics. Compared with ECMs, EMs [15] have rapidly evolved because they can give insight into the battery's physicochemical processes from a microscopic perspective, which is more advantageous for monitoring the battery SOC accurately. Nevertheless, the heavy computational expense of EM has made its use in practical applications challenging. As a result, reduced-order EMs [16–18] used for battery SOC estimation have gradually become mainstream. For instance, Lin et al. [19] estimated SOC with EKF algorithm based

on a single particle model (SPM) for lithium-ion batteries, while linearization was carried out at each time step when using EKF, which increased the computational burden and inevitable errors. Tanim [20] and Moura [21] achieved the SOC estimation by using state observers based on an enhanced single particle model (ESPM). Nevertheless, conventional microcomputers in BMS cannot support observations based on complex mathematical derivations, which means that such approaches cannot achieve the online estimation well in actual conditions.

In addition, it is reported that the current sensor bias [22] has a serious impact on the accuracy of SOC estimation. To deal with this problem, Dai et al. [23] selected an adaptive variable multi-timescale framework to realize the co-estimation of battery SOC and SOH for eliminating the current measurement offset. Hosny et al. [24] applied a non-linear Kalman filter to an augmented model for reducing the influence of the biases in measurements on battery SOC estimation. However, these approaches were only carried out in ECMs, while sensor bias was rarely considered in existing EMs-based SOC estimation methods.

Since the platforms of BMS in EVs for implementing the estimation algorithms are generally low-cost microcontrollers, the computational power and resources are usually limited. For this reason, the proportional–integral observers (PIOs) [25–27] have attracted extensive attention recently due to its applicability to online estimation. Meanwhile, the PIO does not involve the complicated mathematical derivation, which brings great potential for its application in EM-based SOC estimation. According to these research foundations, this paper proposes an online SOC estimation based on simplified EM for LIB considering current sensor bias. In EM-based SOC estimation structure, the errors from current sensor bias are considered by PIO. Then, the accuracy of SOC estimation is validated under different operating conditions.

This paper is organized as follows. Section 2 describes a simplified EM for LIBs. Section 3 proposes an online SOC estimation based on simplified EM for LIBs, considering current sensor bias. Simulations and experimental verification on the accuracy of SOC estimation are shown in Section 4. Conclusions are given in Section 5.

## 2. Derivation of the Simplified EM

Although the full order EMs (i.e., P2D model) have been widely used in the performance simulation and design optimization of batteries, they become a major obstacle in real-time computation for battery models because of the highly nonlinear governing equations. In order to realize the EMs on-board application in control fields, an improved reduced-order EM for lithium-ion batteries needs to be reconstructed. A more comprehensive understanding of the governing equations and meanings of related parameters for simplified EMs has been shown in our previous work [28]. For this reason, the reconstruction process of a simplified EM is only briefly explained as follows. As shown in Figure 1, solid phases in anode and cathode electrodes are represented by two particles in the simplified EM. It is emphasized that there is an assumption that the reaction current density on the entire electrode is evenly distributed, and the average pore wall flux of lithium ions at two current collectors are, respectively, computed as:

$$J_p = -\frac{i_{app}}{a_p FL_p} \quad (1)$$

$$J_n = +\frac{i_{app}}{a_n FL_n} \quad (2)$$

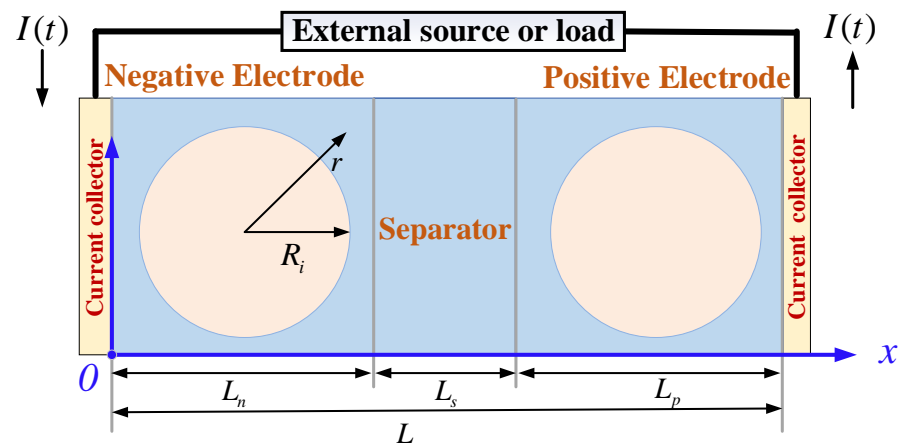


Figure 1. Schematic of the simplified EM for LIB.

### 2.1. Solid Phase Diffusion Process

In this section, the solid phase equations are solved in a novel hybrid approach for ensuring computational efficiency and better observability. That is to say, the quadratic-parameter parabolic approach [29] is employed to calculate the concentration distribution in a positive electrode, and the third order Padé approximation [30] is used to calculate the concentration distribution in a negative electrode.

For the solid phase equations of a negative electrode, we can get a state-space equation form as:

$$\begin{cases} \dot{\mathbf{x}} = \mathbf{A}\mathbf{x} + \mathbf{B}i_{app} \\ \mathbf{y} = \mathbf{C}\mathbf{x} \end{cases} \quad (3)$$

$$\mathbf{y} = [c_{s,n,surf} \quad \bar{c}_{s,n}]^T \quad (4)$$

It is noted that the output vector  $\mathbf{y}$  has a line combination with the system states vector  $\mathbf{x} = [x_1, x_2, x_3]^T$  and the coefficient matrices  $\mathbf{A}$ ,  $\mathbf{B}$ ,  $\mathbf{C}$  for the third-order form are listed below:

$$\mathbf{A} = \begin{bmatrix} 0 & 1 & 0 \\ 0 & 0 & 1 \\ 0 & -\frac{3456(D_{s,n})^2}{R_p^4} & -\frac{189D_{s,n}}{R_p^4} \end{bmatrix}, \quad \mathbf{B} = \left[ 0 \quad 0 \quad \frac{1}{L_n} \right]^T$$

$$\mathbf{C} = \left[ -\frac{10395(D_{s,n})^2}{a_n F (R_n)^5} \quad -\frac{1260D_{s,n}}{a_n F (R_n)^3} \quad -\frac{21}{a_n F R_n}; \quad -\frac{10395(D_{s,n})^2}{a_n F (R_n)^5} \quad -\frac{252D_{s,n}}{a_n F (R_n)^3} \quad -\frac{3}{a_n F R_n} \right]$$

For the solid phase equations of a positive electrode, we can get the ordinary-differential equations as:

$$\frac{d\bar{c}_{s,p}(t)}{dt} = -\frac{3}{R_p} \frac{i_{app}}{F a_p L_p} \quad (5)$$

$$\bar{c}_{s,p,surf}(t) = \bar{c}_{s,p}(t) - \frac{i_{app} R_p}{5D_{s,p} F a_p L_p} \quad (6)$$

Though the quadratic-parameter parabolic may sacrifice some precision to a certain extent, this has almost no effect on the open circuit voltage of an electrode. On the contrary, this novel hybrid approach can improve the observability of the LIBs system, as well as guarantee computational efficiency. It is emphasized that this simplification approach of the solid phase equations, such as Equations (3) and (4), has good accuracy in solid surface concentration and less impact on subsequent EM-based SOC estimation at medium/high C-rates, which has been described and verified in Ref. [28].

## 2.2. Electrolyte Diffusion Process

SPM manifests a poor precision under high C-rates as it ignores the electrolyte dynamics. As a result, the reduced-order EM with the simplified electrolyte concentration distribution has drawn much attention.

In order to describe the electrolyte diffusion process with an acceptable computational efficiency and accuracy, the volume-averaged forms of the equations for electrolyte diffusion are obtained as follows [31]:

$$c_{e,n}(x, t) = c_{2in}(t) + \frac{q_{2in}}{2L_n D_{e,n}^{eff}} (L_n^2 - x^2) \quad (7)$$

$$c_{e,s}(x, t) = c_{2in}(t) - \frac{q_{2in}(t)}{D_{e,s}^{eff}} (x - L_n) + \left( \frac{q_{2in}(t) - q_{2ip}(t)}{L_s D_{e,s}^{eff}} \right) \frac{(x - L_n)^2}{2} \quad (8)$$

$$c_{e,p}(x, t) = c_{2ip}(t) - \frac{q_{2ip}(t)}{2L_p D_{e,p}^{eff}} [L_p^2 - (L - x)^2] \quad (9)$$

Finally, the electrolyte concentration of the positive and negative electrodes at the current collector interface can be calculated as:

$$c_{e,n}(0, t) = c_{2in}(t) + \frac{q_{2in}(t)}{2D_{e,n}^{eff}} L_n \quad (10)$$

$$c_{e,p}(L, t) = c_{2ip}(t) - \frac{q_{2ip}(t)}{2D_{e,p}^{eff}} L_p \quad (11)$$

It is noted that the detailed expressions of  $c_{2ip}(t)$ ,  $c_{2in}(t)$ ,  $q_{2ip}(t)$ ,  $q_{2in}(t)$ , can be found in [31].

## 2.3. Cell Terminal Output Voltage

For the cell terminal output voltage (TOV), it is commonly defined as the difference between the potential at negative and positive current collectors:

$$V_{cell}(t) = \Phi_s(L, t) - \Phi_s(0, t) \quad (12)$$

where  $\Phi_s(x, t)$  is the solid phase potential of an electrode.  $V_{cell}(t)$  is the time varying TOV of a LIB.

According to the governing equations of over potential, the Equation (12) can be rearranged as:

$$V_{cell}(t) = OCV_{cell} + \eta_e + \eta_{kin} + \eta_{ohm} \quad (13)$$

where  $OCV_{CELL}$  is the open circuit voltage of battery,  $\eta_e$  is the electrolyte over potential,  $\eta_{kin}$  is the kinetics reaction overpotential and  $\eta_{ohm}$  is the over potential caused by the resistance of solid electrolyte interface film. At the same time, the expressions of each part can be calculated as detailed in Ref. [32] and shown as:

$$OCV_{cell} = U_p \left[ \frac{c_{s,p,surf}(t)}{c_{s,p,max}} \right] - \left[ \frac{c_{s,n,surf}(t)}{c_{s,n,max}} \right] \quad (14)$$

$$\eta_e = \varphi_e(L, t) - \varphi_e(0, t) = (1 - t_+) \frac{2RT}{F} \ln \frac{c_e(L, t)}{c_e(0, t)} - \frac{i_{app}}{2} \left( \frac{L_n}{k_n^{eff}} + \frac{2L_s}{k_s^{eff}} + \frac{L_p}{k_p^{eff}} \right) \quad (15)$$

$$\eta_{kin} = \frac{2RT}{F} \left\{ \ln \left[ m_p(t) + \sqrt{m_p^2(t) + 1} \right] - \ln \left[ m_n(t) + \sqrt{m_n^2(t) + 1} \right] \right\} \quad (16)$$

$$\eta_{ohm} = -R_f i_{pp} \quad (17)$$

where  $m_i(t) = \frac{i_{app}}{2i_{0,i}}$ ,  $i_{0,i}$  is the exchange current density,  $R_f$  represents the resistance of battery film contact  $U_p$ , and  $U_n$  are the open circuit voltage at positive and negative electrodes.

### 3. SOC Estimation with PI Observer

In the current EV applications, the current sensor bias is usually regarded as a severe fault in many control algorithms of BMS [23]. As the current is an important input to a battery model, the current sensor bias will influence the transferred charge and inevitably contribute to the inaccurate SOC estimation of a battery. To this end, a PI observer is herein designed to compensate for the current sensor bias, and this is a simple but practical approach to EM-SOC estimation. Different from the previous research [25–27], the novelty of this paper is that the online SOC estimation is carried out based on simplified EMs for LIBs, which can provide a more acceptable estimation accuracy, as well as a better observation of the internal states for a LIB cell. It is noted that the influence of current rates and temperature on EM-based SOC is ignored in this paper. Meanwhile, battery aging is also not within the scope of our discussion.

#### 3.1. Proportional-Integral Observer

In order to deal with the current sensor bias and accurately monitor the battery SOC status in real time, a traditional PI observer is designed, and its expression is shown [25]:

$$G_I = K_p \cdot \left( \Delta U + \frac{1}{T_i} \cdot \sum_{i=0}^k \Delta U \right) \quad (18)$$

where  $G_I$  is the feedback quantity for current compensation,  $K_p$  represents the proportional gain and  $1/T_i$  represents the integration gain.

Here,  $\Delta U$  is defined as the model error, which is real-time difference between the battery TOV of simplified EM based PI observer (TOV\_PIO) and the TOV of the real battery (TOV\_exp) and combined with the Equation (13), the model error  $\Delta U$  is expressed as:

$$\Delta U = \text{TOV\_exp} - \text{TOV\_PIO} = \text{TOV\_exp} - \text{OCV}_{cell} - \eta_e - \eta_{kin} - \eta_{ohm} \quad (19)$$

Then, according to the feedback quantity  $G_I$  of PI observer, the input current of the battery EM  $i_{mod}$  is corrected and fed back to the solid phase diffusion process so that the solid phase surface concentration  $\bar{c}_{s,n}(t)$  related to SOC is updated by Equations (3) and (4). Defining the  $i_{exp}$  as real charging/discharging current, thus the specific expressions are as follows:

$$i_{mod} = i_{exp} + G_I = i_{exp} + K_p \cdot \left( \Delta U + \frac{1}{T_i} \cdot \sum_{i=0}^k \Delta U \right) \quad (20)$$

$$\bar{c}_{s,n}(t) = f(i_{mod}) \quad (21)$$

Here, the detailed relationship between the input current  $i_{mod}$  and the solid phase surface concentration  $\bar{c}_{s,n}(t)$  can be found in Equations (3) and (4).

#### 3.2. Framework of EM-Based SOC Estimation

Combined with the above analysis of PI observer, the framework of the proposed SOC estimation is given in Figure 2. As shown in Figure 2, the adopted battery model is simplified EM described in Section 2, which can improve the observability of the LIBs system, as well as guarantee computational efficiency. Additionally, the verified COMSOL results [33] here are defined as the experimental TOV of the real battery without current sensor error, subjected to charging/discharging current  $i_{exp}$ .

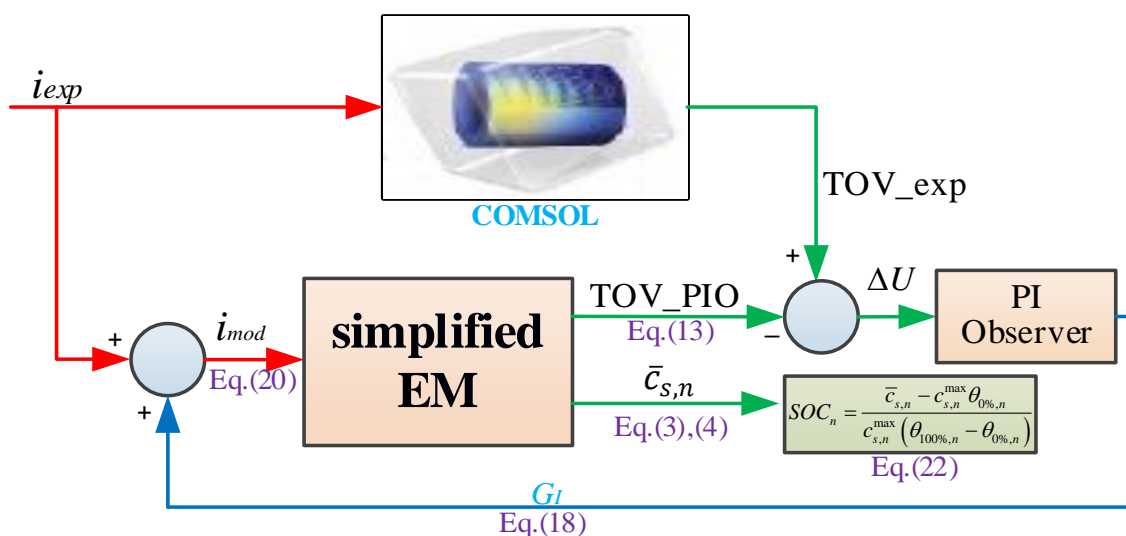


**Figure 2.** Framework of the proposed SOC estimation.

In practice, the TOV\_PIO is different from the TOV\_exp owing to the sensor external disturbance. According to introducing the PI observer, the  $\Delta U$  combined with observer gain is used to compensate the input current with disturbance and allow it to become the corrected current  $i_{mod}$ . On the other hand, the battery simplified EM receives the corrected current  $i_{mod}$ , then it estimates the solid surface concentration  $\bar{c}_{s,n}(t)$  and the TOV\_PIO in real time. Specifically, the value of TOV\_PIO is calculated by Equation (13), and solid surface concentration  $\bar{c}_{s,n}$  is updated by Equations (3) and (4). In this case, the battery SOC characterizing the electrochemical meaning can be calculated as [34]:

$$SOC = \frac{\bar{c}_{s,n} - c_{s,n}^{\max} \theta_{0\%,n}}{c_{s,n}^{\max} (\theta_{100\%,n} - \theta_{0\%,n})} \quad (22)$$

where  $\theta_{0\%,n}$  is the reference stoichiometric number of a negative electrode at 0% SOC, and  $\theta_{100\%,n}$  is the reference stoichiometric number of a negative electrode at 100% SOC.

Considering that the surface concentration of solid phase is related to the side reactions in the battery [35], it should be noted that here the  $c_{s,p,surf}$  used is replaced by  $\bar{c}_{s,n}$  to calculate the battery SOC, which can better ensure the battery charging and discharging safety.

#### 4. Results and Discussion

In this section, the effectiveness of the proposed simplified EM and accuracy of SOC estimation are investigated against the verified COMSOL results defined as the experimental data of the real battery. The LiyMn2O4-LixC6 battery is used for simulation and verification, whose values of parameters are given in [28]. In addition, it should be noted that all simulations and verifications in this paper are implemented under isothermal conditions.

##### 4.1. Validation of Simplified EM

For the model based SOC estimation, the accuracy of the model has an important impact on the accuracy of SOC estimation. For this reason, the performance evaluation for TOV of simplified EM should firstly be carried out at the galvanostatic discharge condition. In this section, the simulation of battery discharge is carried out at the constant current of 0.5 C, 1 C, 2 C, 4 C, respectively.

Figure 3 shows a comparison of simulated discharge curves between simplified EM and the Newman model [15]. It can be observed that the simulated results from simplified EM accord well with that from the Newman model, especially at low and medium C-rates. This significantly good degree of agreement is attributed to considering the variations of electrolyte potential in proposed the simplified EM. From the validation results, although it

is not as good as the reduced-order of the full P2D model [36], this simplified EM in model fidelity can accurately predict the TOVs under a certain range of discharge rates (0.5 C–4 C) in a sampling time of seconds and has a certain advantage in computing efficiency for online application [28], which lays the foundation for accurate SOC estimation in the next section.

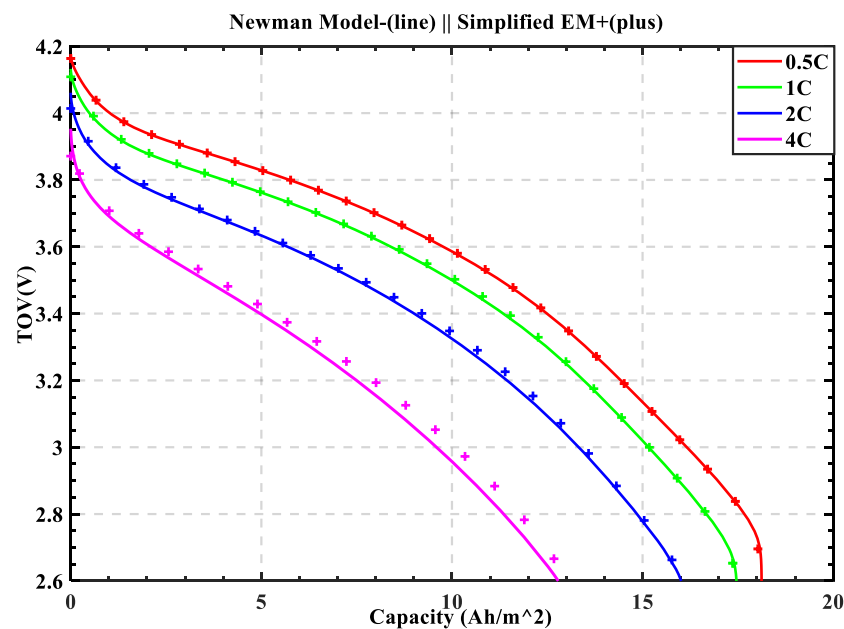
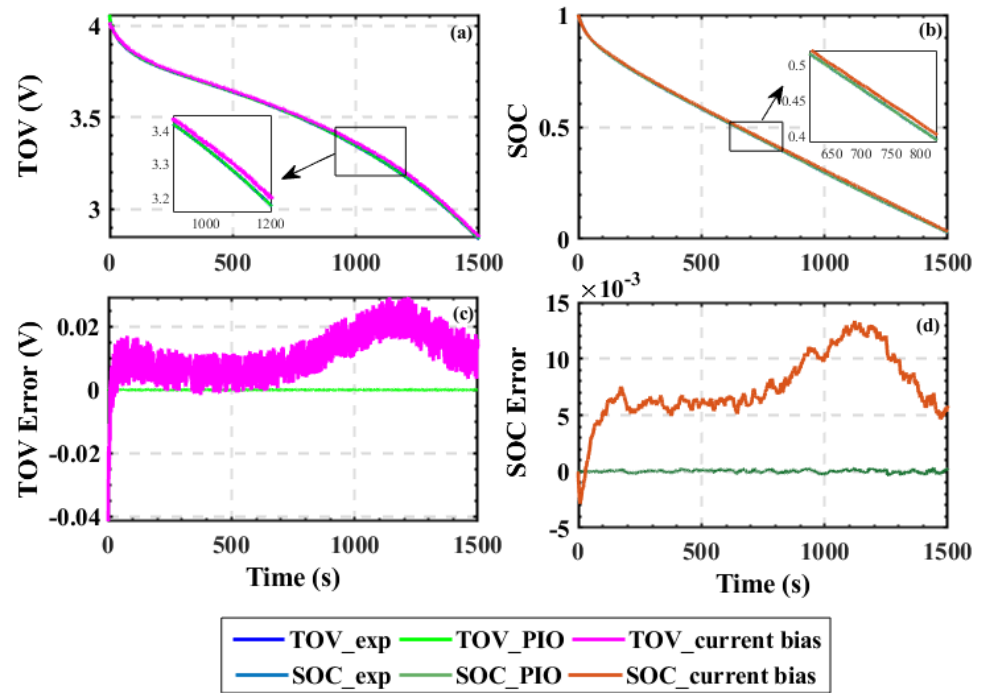


Figure 3. Performance evaluation for battery TOV under different C-rates.

#### 4.2. Evaluation of SOC Estimation

The performance of SOC estimation based on PI observer is examined by comparing the actual SOC in experimental validation tests. The actual SOC as the reference value obtained by the integral of current over time, using the Coulomb counting method. It is worth noting that, for the constant current and dynamic condition, the current sensor bias is set to a uniformly distributed random signal with a range of  $[-2, 2]$  A/m<sup>2</sup> and sampling time for the current sensor bias is one second. Furthermore, in order to better evaluate the correction performance of the current, the initial SOC is set to 100% correctly. At the same time, the variables used in the verification process are explained as: the TOV/SOC\_exp are experimental TOV/SOC without current sensor bias, the TOV/SOC\_PIO are corrected TOV/SOC considering the current sensor bias and the TOV/SOC\_current bias are uncorrected TOV/SOC considering the current sensor bias. It should be noted that the TOV/SOC errors in the figures are defined as the difference between the TOV/SOC\_exp and TOV/SOC\_PIO, or the difference between the TOV/SOC\_exp and TOV/SOC\_current bias. Figure 4 shows the estimation results of the model TOV and SOC, considering sensor bias at 2 C-rates condition. It can be seen from Figure 4c,d that the current sensor bias has led to an inaccurate estimation of battery TOV and SOC. Specifically, TOV error fluctuates between  $-0.04$  V and  $0.03$  V as the change of current bias. In addition, the SOC error is as high as 0.015 at 1200 s. Although these errors present a small order of magnitude, it will make the battery system unstable. By contrast, TOV and SOC estimation based on PI observer are consistent with the real experiment values, whose errors are almost kept at zero value. Accordingly, the proposed SOC estimation can eliminate current sensor errors to some extent and show good performance under the constant current condition.



**Figure 4.** Estimation results of the model TOV and SOC considering sensor bias at 2 C condition. (a) Results of TOV, (b) Results of SOC, (c) Errors of TOV, (d) Errors of SOC.

To further assess the accuracy of SOC estimation under the dynamic condition, Figures 5 and 6 present the estimation results of the model TOV and SOC, considering sensor bias under the Dynamic Stress Test (DST) condition, respectively. As depicted in Figure 5b,c, the estimation of TOV based on PIO can well eliminate the influence of current bias and TOV is, overall, accorded with the real experiment values. However, the estimation of TOV without PIO fluctuates greatly due to the influence of current bias and its TOV error is kept in ±0.05 V. Additionally, according to the Figure 6b,c, SOC estimation based on PIO also reduces the influence of current bias to some extent and presents a good accuracy under DST condition.

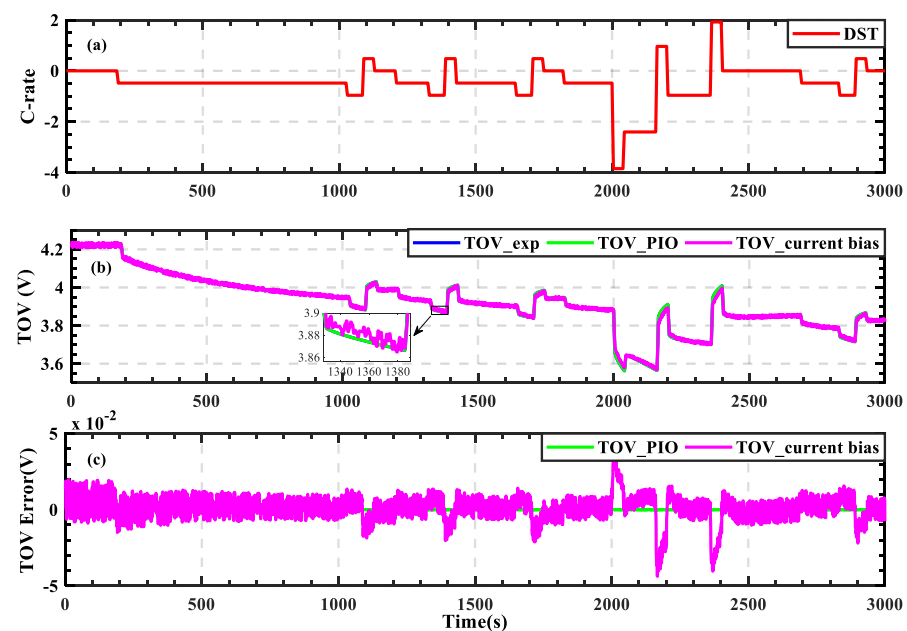


**Figure 5.** Estimation results of the model TOV considering current bias under DST condition. (a) DST profile, (b) Results of TOV, (c) Errors of TOV.

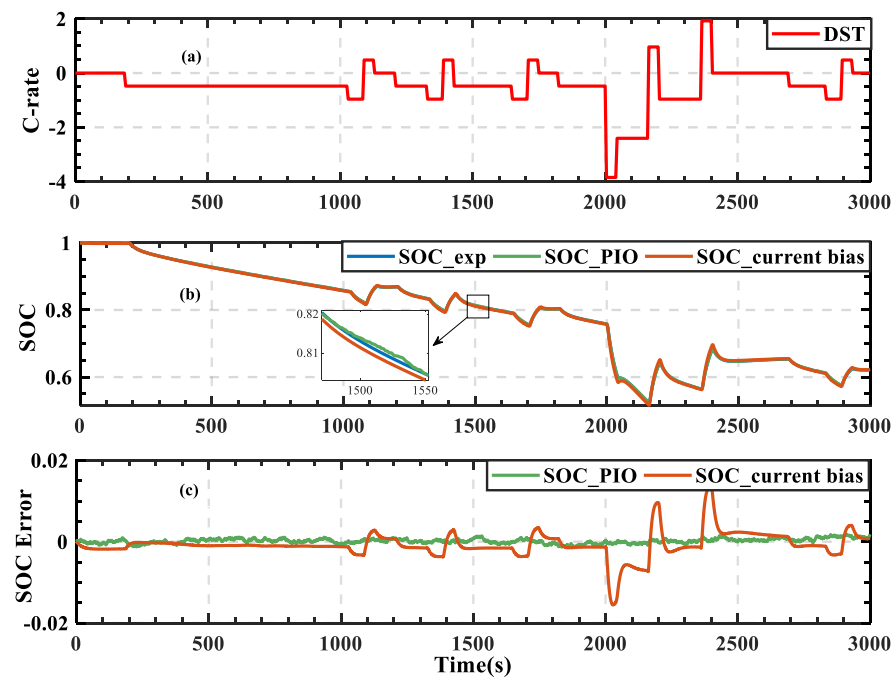


**Figure 6.** Estimation results of SOC considering current bias under DST condition. (a) DST profile, (b) Results of SOC, (c) Errors of SOC.

In order to give a quantitative evaluation on the performance of the proposed methods based on PI observer, the max error (MaxE) and the root mean squared error (RMSE) for estimated results of TOV/SOC under 2 C-rates and DST conditions are listed in Table 1. Here, the selected evaluation criteria for TOV/SOC estimation are calculated by:

$$\text{MaxE} = \text{Max} |Y_k - \hat{Y}_k| \quad (23)$$

$$\text{RMSE} = \sqrt{\frac{1}{n} \sum_{k=1}^n (Y_k - \hat{Y}_k)^2} \quad (24)$$

where  $Y$  includes the real TOV\_exp and SOC\_exp,  $\hat{Y}$  includes the estimated TOV\_PIO and SOC\_PIO,  $k$  represents the  $k$ th point of sampling time and  $n$  is total number of sampling time points during the simulation.

**Table 1.** Results of the TOV/SOC errors based on PIO.

	MaxE		RMSE	
	TOV_PIO (mV)	SOC_PIO (%)	TOV_PIO (mV)	SOC_PIO (%)
2 C	0.28	0.34	0.05	0.01
DST	0.33	0.18	0.05	0.06

As shown from the Table 1, under 2 C condition, the MaxE of TOV is just 0.28 mV and the RMSE of the TOV is 0.05 mV. For the SOC estimation, the MaxE and RMSE is 0.34% and 0.01% respectively. On the other hand, the influence of current sensor bias under DST condition is reduced as well as estimations of TOV and SOC also present good accuracy, whose MaxEs are 0.33 mV and 0.18%. It should be noted that the estimation accuracy of TOV and SOC depends on the degree of current sensor bias.

Based on the above discussion and the experimental validation, the PI observer based on simplified EM can well estimate battery SOC and voltage. In addition, the impact of current sensor bias on battery SOC estimation can be eliminated under different operation situations.

## 5. Conclusions

In this paper, an online SOC estimation approach based on a simplified EM for lithium-ion batteries considering sensor bias is proposed. By using the reduced order techniques for equations in solid and liquid phases, a simplified EM is reconstructed and verified. Then, a PI observer is designed to eliminate the influence of current sensor bias and estimate the battery TOV and SOC under different conditions. Specifically, under 2 C and DST conditions, the MaxEs of TOV are only 0.28 mV and 0.33 mV, respectively. For the SOC estimation, the MaxEs of that are only 0.34% and 0.18%. These experiment results indicate that the proposed method has a good performance in both estimation accuracy and computing efficiency, even if there exists the current bias, which facilitates the on-board application in BMS.

Considering the impact of current rates and temperature on model parameters, the electrochemical-thermal model will be explored and the influence of temperature on SOC estimation will also be further investigated in future work.

**Author Contributions:** Conceptualization, methodology, and validation, L.W.; formal analysis, J.J.; resources, K.L. and H.P.; data curation, J.J.; writing—original draft preparation, L.W.; writing—review and editing, H.P. All authors have read and agreed to the published version of the manuscript.

**Funding:** This research was funded by National Natural Science Foundation of China (NO.51675423).

**Institutional Review Board Statement:** Not applicable.

**Informed Consent Statement:** Not applicable.

**Data Availability Statement:** Not applicable.

**Acknowledgments:** The authors gratefully acknowledge the support of National Natural Science Foundation of China (NO.51675423) and International Conference on Electric and Intelligent Vehicles 2021.

**Conflicts of Interest:** The authors declare no conflict of interest.

## Nomenclature

$a_i$	specific surface area [ $\text{m}^{-1}$ ]
$A$	electrode surface area [ $\text{m}^3$ ]
$c_{s,i,surf}$	solid-phase surface concentration [ $\text{mol m}^{-3}$ ]
$c_{s,i}^{max}$	maximum lithium-ion concentration [ $\text{mol m}^{-3}$ ]
$c_{e,i}$	electrolyte concentration [ $\text{mol m}^{-3}$ ]
$\bar{c}_{s,i}$	average solid-phase concentration [ $\text{mol m}^{-3}$ ]
$c_{2in}$	electrolyte concentration at the interface between the negative electrode and the separator [ $\text{mol m}^{-3}$ ]
$c_{2ip}$	electrolyte concentration at the interface between the positive at the electrode and the separator [ $\text{mol m}^{-3}$ ]
$D_e$	electrolyte diffusion coefficient [ $\text{m}^2 \text{s}^{-1}$ ]
$c_{e,i}^{eff}$	effective electrolyte diffusion coefficient [ $\text{m}^2 \text{s}^{-1}$ ]
$D_{s,i}$	solid-phase diffusion coefficient [ $\text{m}^2 \text{s}^{-1}$ ]
$F$	Faraday constant [ $96,487 \text{ C mol}^{-1}$ ]
$i_{app}$	applied current density [ $\text{A m}^{-2}$ ]
$i_{0,i}$	exchange current density [ $\text{A m}^{-2}$ ]
$J_i$	pore wall flux [ $\text{mol m}^{-2} \text{s}^{-1}$ ]
$L_i$	thickness of porous regions [m]
$q_{2in}$	diffusion flux at the interface of the negative electrode and separator [ $\text{mol m}^{-2} \text{s}^{-1}$ ]
$q_{2ip}$	diffusion flux at the interface of the positive electrode and separator [ $\text{mol m}^{-2} \text{s}^{-1}$ ]
$R$	universal gas constant [ $8.314 \text{ J mol}^{-1} \text{ K}^{-1}$ ]
$R_f$	resistance of battery film contact [ $\Omega$ ]
$R_i$	particle radius of electrodes [m]
$t_+$	electrolyte transference number
$T$	battery temperature [K]

## Subscripts

<i>i</i>	substitution of <i>n</i> , <i>sep</i> or <i>p</i>
<i>n</i>	negative electrode
<i>p</i>	positive electrode
<i>s</i>	separator

## References

- Rahimi-Eichi, H.; Ojha, U.; Baronti, F.; Chow, M.-Y. Battery Management System: An Overview of Its Application in the Smart Grid and Electric Vehicles. *IEEE Ind. Electron. Mag.* **2013**, *7*, 4–16. [\[CrossRef\]](#)
- Wei, Z.; Zhao, J.; He, H.; Ding, G.; Cui, H.; Liu, L. Future smart battery and management: Advanced sensing from external to embedded multi-dimensional measurement. *J. Power Sources* **2021**, *489*, 229462. [\[CrossRef\]](#)
- Xiong, R.; Wang, J.; Shen, W.; Tian, J.; Mu, H. Co-Estimation of State of Charge and Capacity for Lithium-ion Batteries with Multi-Stage Model Fusion Method. *Engineering* **2021**, in press. [\[CrossRef\]](#)
- Boulmrharj, S.; Ouladsine, R.; NaitMalek, Y.; Bakhouya, M.; Zine-Dine, K.; Khaidar, M.; Siniti, M. Online battery state-of-charge estimation methods in micro-grid systems. *J. Energy Storage* **2020**, *30*, 101518. [\[CrossRef\]](#)
- Pang, H.; Guo, L.; Wu, L.; Jin, X. An enhanced temperature-dependent model and state-of-charge estimation for a Li-Ion battery using extended Kalman filter. *Int. J. Energy Res.* **2020**, *44*, 7254–7267. [\[CrossRef\]](#)
- Wang, S.; Fernandez, C.; Shang, L.; Li, Z.; Li, J. Online state of charge estimation for the aerial lithium-ion battery packs based on the improved extended Kalman filter method. *J. Energy Storage* **2017**, *9*, 69–83. [\[CrossRef\]](#)
- Farag, M.; Fleckenstein, M.; Habibi, S. Continuous piecewise-linear, reduced-order electrochemical model for lithium-ion batteries in real-time applications. *J. Power Sources* **2017**, *342*, 351–362. [\[CrossRef\]](#)
- Pang, H.; Mou, L.; Guo, L.; Zhang, F. Parameter identification and systematic validation of an enhanced single-particle model with aging degradation physics for Li-ion batteries. *Electrochim. Acta* **2019**, *307*, 474–487. [\[CrossRef\]](#)
- Plett, G.L. Extended Kalman filtering for battery management systems of LiPB-based HEV battery packs: Part 3. State and parameter estimation. *J. Power Sources* **2004**, *134*, 277–292. [\[CrossRef\]](#)
- Li, W.; Yang, Y.; Wang, D.; Yin, S. The multi-innovation extended Kalman filter algorithm for battery SOC estimation. *Ionics* **2020**, *26*, 6145–6156. [\[CrossRef\]](#)
- Yu, Q.; Wan, C.; Li, J.; Zhang, X.; Huang, Y.; Liu, T. An Open Circuit Voltage Model Fusion Method for State of Charge Estimation of Lithium-Ion Batteries. *Energies* **2021**, *14*, 1797. [\[CrossRef\]](#)
- Ceraolo, M.; Lutzemberger, G.; Poli, D.; Scarpelli, C. Luenberger-based State-Of-Charge evaluation and experimental validation with lithium cells. *J. Energy Storage* **2020**, *30*, 101534. [\[CrossRef\]](#)
- Hu, X.; Sun, F.; Zou, Y. Estimation of State of Charge of a Lithium-Ion Battery Pack for Electric Vehicles Using an Adaptive Luenberger Observer. *Energies* **2010**, *3*, 1586–1603. [\[CrossRef\]](#)
- Chen, X.; Shen, W.; Cao, Z.; Kapoor, A. A novel approach for state of charge estimation based on adaptive switching gain sliding mode observer in electric vehicles. *J. Power Sources* **2014**, *246*, 667–678. [\[CrossRef\]](#)
- Doyle, M.; Newman, J.; Gozdz, A.S.; Schmutz, C.N.; Tarascon, J. Comparison of Modeling Predictions with Experimental Data from Plastic Lithium Ion Cells. *J. Electrochem. Soc.* **1996**, *143*, 1890–1903. [\[CrossRef\]](#)
- Tian, J.; Wang, Y.; Chen, Z. An improved single particle model for lithium-ion batteries based on main stress factor compensation. *J. Clean. Prod.* **2021**, *278*, 123456. [\[CrossRef\]](#)
- Zou, C.; Hu, X.; Wei, Z.; Wik, T.; Egardt, B. Electrochemical Estimation and Control for Lithium-Ion Battery Health-Aware Fast Charging. *IEEE Trans. Ind. Electron.* **2017**, *65*, 1–11. [\[CrossRef\]](#)
- Li, J.; Wang, L.; Lyu, C.; Liu, E.; Xing, Y.; Pecht, M. A parameter estimation method for a simplified electrochemical model for Li-ion batteries. *Electrochim. Acta* **2018**, *275*, 50–58. [\[CrossRef\]](#)
- Lin, C.; Tang, A.; Xing, J. Evaluation of electrochemical models based battery state-of-charge estimation approaches for electric vehicles. *Appl. Energy* **2017**, *207*, 394–404. [\[CrossRef\]](#)
- Tanim, T.R.; Rahn, C.D.; Wang, C.Y. State of charge estimation of a lithium-ion cell based on a temperature dependent and electrolyte enhanced single particle model. *Energy* **2015**, *80*, 731–739. [\[CrossRef\]](#)
- Moura, S.J.; Chaturvedi, N.A.; Krstić, M. Adaptive partial differential equation observer for battery state-of-charge/state-of-health estimation via an electrochemical model. *J. Dyn. Syst. Meas. Control* **2014**, *136*, 011015. [\[CrossRef\]](#)
- Zheng, Y.; Ouyang, M.; Han, X.; Lu, L.; Li, J. Investigating the error sources of the online state of charge estimation methods for lithium-ion batteries in electric vehicles. *J. Power Sources* **2018**, *377*, 161–188. [\[CrossRef\]](#)
- Jiang, B.; Dai, H.; Wei, X.; Xu, T. Joint estimation of lithium-ion battery state of charge and capacity within an adaptive variable multi-timescale framework considering current measurement offset. *Appl. Energy* **2019**, *253*, 113619. [\[CrossRef\]](#)
- Al-Gabalawy, M.; Hosny, N.S.; Dawson, J.A.; Omar, A. State of charge estimation of a Li-ion battery based on extended Kalman filtering and sensor bias. *Int. J. Energy Res.* **2021**, *45*, 6708–6726. [\[CrossRef\]](#)
- Meng, J.; Ricco, M.; Acharya, A.B.; Luo, G.; Swierczynski, M.; Stroe, D.-I.; Teodorescu, R. Low-complexity online estimation for LiFePO<sub>4</sub> battery state of charge in electric vehicles. *J. Power Sources* **2018**, *395*, 280–288. [\[CrossRef\]](#)
- Xu, J.; Mi, C.; Cao, B.; Deng, J.; Chen, Z.; Li, S. The State of Charge Estimation of Lithium-Ion Batteries Based on a Proportional-Integral Observer. *IEEE Trans. Veh. Technol.* **2014**, *63*, 1614–1621. [\[CrossRef\]](#)

27. Tang, X.; Wang, Y.; Chen, Z. A method for state-of-charge estimation of LiFePO<sub>4</sub> batteries based on a dual-circuit state observer. *J. Power Sources* **2015**, *296*, 23–29. [[CrossRef](#)]
28. Wu, L.; Liu, K.; Pang, H. Evaluation and observability analysis of an improved reduced-order electrochemical model for lithium-ion battery. *Electrochim. Acta* **2021**, *368*, 137604. [[CrossRef](#)]
29. Li, C.; Cui, N.; Wang, C.; Zhang, C. Reduced-order electrochemical model for lithium-ion battery with domain decomposition and polynomial approximation methods. *Energy* **2021**, *221*, 119662. [[CrossRef](#)]
30. Zhao, Y.; Choe, S.Y. A highly efficient reduced order electrochemical model for a large format LiMn<sub>2</sub>O<sub>4</sub>/Carbon polymer battery for real time applications. *Electrochim. Acta* **2015**, *164*, 97–107. [[CrossRef](#)]
31. Kumar, V.S. Reduced order model for a lithium-ion cell with uniform reaction rate approximation. *J. Power Sources* **2013**, *222*, 426–441. [[CrossRef](#)]
32. Prada, E.; Di Domenico, D.; Creff, Y.; Bernard, J.C.; Sauvante-Moynot, V.; Huet, F. Simplified Electrochemical and Thermal Model of LiFePO<sub>4</sub>-Graphite Li-Ion Batteries for Fast Charge Applications. *J. Electrochem. Soc.* **2012**, *159*, A1508–A1519. [[CrossRef](#)]
33. Cai, L.; White, R.E. Mathematical modeling of a lithium-ion battery with thermal effects in COMSOL Inc. Multiphysics (MP) software. *J. Power Sources* **2011**, *196*, 5985–5989. [[CrossRef](#)]
34. Fan, G.; Li, X.; Zhang, R. Global Sensitivity Analysis on Temperature-Dependent Parameters of a Reduced-Order Electrochemical Model and Robust State-of-Charge Estimation at Different Temperatures. *Energy* **2021**, *223*, 120024. [[CrossRef](#)]
35. Li, W.; Fan, Y.; Ringbeck, F.; Jöst, D.; Han, X.; Ouyang, M.; Sauer, D.U. Electrochemical model-based state estimation for lithium-ion batteries with adaptive unscented Kalman filter. *J. Power Sources* **2020**, *476*, 228534. [[CrossRef](#)]
36. Han, S.; Tang, Y.; Rahimian, S.K. A numerically efficient method of solving the full-order pseudo-2-dimensional (P2D) Li-ion cell model. *J. Power Sources* **2021**, *490*, 229571. [[CrossRef](#)]